Multidisciplinary Performance Enhancement on a Fixed-wing Unmanned Aerial Vehicle via Simultaneous Morphing Wing and Control System Design

Yüksel Eraslan

Iskenderun Vocational School of Higher Education, Iskenderun Technical University, Hatay 31280, Türkiye; e-mail: yuksel.eraslan@iste.edu.tr

Tuğrul Oktay

Faculty of Aeronautics and Astronautics, Erciyes University, Kayseri 38280, Türkiye; e-mail: oktay@erciyes.edu.tr

Corresponding author: yuksel.eraslan@iste.edu.tr

Aerial vehicle design process usually aims to maximize performance in a specific flight phase regarding a particular topic such as aerodynamics, flight qualities, or control. This paper proposes a multidisciplinary enhancement both in aerodynamics and longitudinal autonomous flight performance (LAFP) via modern simultaneous design methodology conducted with a novel morphing idea. In this regard, the main wing of a fixed-wing unmanned aerial vehicle (UAV) is redesigned with wingtips capable of altering its taper ratio which results in a semi-tapered planform. The dynamic model of morphing aircraft is constituted from data obtained by numerical and analytical approaches for a number of morphing scenarios. The LAFP is identified as the sum of trajectory tracking parameters which are rise time, settling time, and maximum overshoot, while aerodynamic performance is defined as lift-to-drag ratio. A hierarchically structured control system is designed and the proportional-integral-differential (PID) controller coefficients and the taper ratio of the morphing wingtip are optimized via the Simultaneous Perturbation Stochastic Approximation (SPSA) algorithm. The k-Nearest Neighbor (k-NN) machine learning algorithm is also conducted to expand the data limited within the investigated range of morphing scenarios so as to have higher accuracy in optimization. Finally, flight simulations of the morphing UAV with optimal wing and control system design are carried out, closed-loop responses are examined in the presence of the von-Karman turbulence model, and the obtained satisfactory results are presented for both disciplines.

KEYWORDS: Aircraft design, morphing wing, aerodynamics, autonomous flight performance, optimization.

1. Introduction

Unmanned aerial systems have been developing rapidly in the last decades concurrent with relevant unmanned technologies in both military and civilian fields of application. The progress in material technologies beginning from traditional materials of aluminum, steel, and titanium to new generation composite materials, shape memory alloys, piezoelectric and piezocomposite materials absolutely play an important role in this development [3,34]. The superior features of modern-day materials in flexibility, reconfigurability, shape memory, and light weightiness have paved the way for morphing technologies that could be mentioned as a new era in aircraft design. The term "morphing" is defined as the ability of an aircraft component structure to be deformed or adapted for a desirable purpose and could be categorized as wing-body adjustment, airfoil adjustment, and active flow control in terms of their application [24]. The goal is typically to obtain the best performance relying on mission requirements by having the most profitable and less costly morphing configuration. The objective of a morphing scenario on an aerial vehicle design might be obtaining an improvement in aerodynamic or flight performance in a particular flight phase [13, 43, 50], an attitude of control response [1, 25], a mission or trajectory-based cost decrement [7, 18, 27], or a combination of various purposes. From aerodynamics and correspondingly flight performance points of view, fixed-wing aerial vehicles have such applications mostly on their main wing in terms of planform, out-of-plane, or airfoil morphing in the literature [36].

The planform geometry of the main wing is determinative on spanwise lift distribution for a fixed-wing aerial vehicle. In this respect, elliptic planform is well-known to have an ideal lift distribution together with the lower bending moment, but its complex surfaces make manufacture difficulties with traditional methods [5,6]. Therefore, tapering planform designs come to the fore by providing lower drag, higher lift and satisfactory lift distribution, and a lower bending moment rather than aerodynamically inefficient rectangular planforms [10]. In application, there are various types of tapering planform designs such as straight-tapered, semi-tapered, or Schuemann and each has different pros and cons [14]. The aforesaid impacts of tapering planforms are attracting scientists to investigate as a potential in morphing applications to obtain an improvement in aerodynamics and correspondingly flight performance.

A morphing aircraft design process starts with conceptual design and includes successive processes such as preliminary and advanced designs, similar to a non-morphing vehicle except for the definition of a morphing scenario serving a purpose at the beginning [14, 35]. The control system design is traditionally carried out independently of the structural and aerodynamic considerations during this process. However, the design procedure that utilizes simultaneous aircraft and control system design proposes more efficient results in the literature [22, 33]. The approach relies on the optimization of desired parameters related to both disciplines.

From the control point of view, the trajectory tracking qualities (i.e., maximum over-shoot, settling time, rise time), could be mentioned as autonomous flight performance metrics, are one of the crucial issues to be considered for new-generation autonomous aerial vehicles. The autonomous flight performance dramatically depends on aircraft dynamic model which includes stability and control derivatives of the vehicle. In the case of a morphing wing design, aircraft dynamic modeling becomes a more challenging task since the excessive number of parameters are naturally affected due to inertial, aerodynamic, and geometrical alterations [4, 9, 11, 16, 41]. The simultaneous design process targeting an improvement in autonomous flight performance with a morphing design requires a complicated dynamic model and control system parameters to be optimized. In such a complex case, stochastic optimization methods could simply provide an efficient solution. In this regard, Simultaneous Perturbation Stochastic Approximation algorithm is known to have successive results in the literature [21, 32, 38].

This paper focuses on investigation of the modern simultaneous design methodology for a novel morphing idea, which is a combination of wing-body and airfoil adjustment, proposing a multidisciplinary improvement in both vehicle aerodynamics and autonomous flight performance. Within the scope of the study, the main wing of a fixed-wing UAV is rede-

signed with a morphing ability that refers to variation in the taper ratio of wingtips, resulting in a semi-tapered planform with higher lift-to-drag ratio (L/D). The morphing wing and a control system involving PID controller is simultaneously designed, where longitudinal PID coefficients and wingtip taper ratio is optimized to improve the LAFP of the vehicle via SPSA algorithm. Computational aerodynamic performance analyses of wings with various wingtip taper ratios within a defined range are carried out to investigate the morphing effects on aircraft flight dynamics. Furthermore, inertial and geometrical effects are assessed and longitudinal equations of motion are presented in state-space representation. The model also included an additional von-Karman turbulence model related to gust condition variables. To have more accurate results in optimization, the k-NN algorithm is conducted to obtain extended aerodynamic, inertial, and geometric data within the constraints. Optimization results are given in detail and longitudinal flight simulations of the vehicle with optimal control system and morphing design is carried out and trajectory tracking results are presented. It is the first time in the literature that the tapering morphing idea on a fixed-wing UAV is discussed with simultaneous design methodology aiming for autonomous flight performance improvement. Moreover, the process is integrated with a stochastic optimization method and a machine learning algorithm as a novel approach.

2. Related Works

Numerous studies have been investigated benefits of various types of morphing aerial vehicle designs in the literature, especially focused on aerodynamical, structural and flight performance improvements. Falcão et al. [12] proposed a servo-actuated morphing wingtip design capable of adapting various flight phases by changing its cant and toe angles and provided improved range, endurance, stall speed, turn radius, and top speed for various flight cases. Numerical approaches to the multidisciplinary behaviors in terms of aerodynamics and structure of the design were applied and the design was optimized for determined purposes via built-in optimization methods of ANSYS. Moreover, a prototype was produced and the feasibility of the design was revealed.

Franco et al. [13] experimentally investigated aerodynamic performance improvement potential on an electro-actively actuated morphing trailing edge design on Airbus A320 aircraft wing design. The wing was scaled and wind-tunnel analyses were performed to assess aerodynamic performances of morphing flap designs especially for takeoff and landing scenarios. A lift enhancement around 4% to 7% and aerodynamic performance improvement around 8% than original design was obtained.

A variable-sweep morphing wing design and a novel morphing decision strategy were presented by Xu et al. [48], that was accurately providing improved cruising performances in different cruising conditions. The main wing of the Firebee UAV was configured varying in sweep angle and wing area and was aerodynamically investigated via DATCOM and optimized with the objective function of cruise efficiency in fuel consumption. The k-Nearest Neighbor algorithm was conducted to established database to decide the optimal configuration for different cruise conditions. The final simulations they performed showed that the morphing strategy they applied resulted in up to 22.4% fuel consumption saving.

Wang et al. [44] proposed honeycomb structure for flexible trailing edge design resulting in a camber morphing wing design. The tapered design was multidisciplinary optimized considering both aerodynamics and structure. The optimized design provided saving in structural weight as approximately 47.1% and improved aerodynamic performance for all flight phases.

Valldosera et al. [42] proposed a camber-morphing airfoil design achieving higher noise emissions and aeroacoustics performance for high-lift conditions at take-off and landing flight phases. After validating the CFD analysis and acoustics predictions they performed on supercritical airfoil NLR 7301 with experimental data, the airfoil was parametrized with Free-Form-Deformation. The optimization process resulted in up to a 22% noise reduction.

Di Luca et al. [8] investigated a bio-inspired wing design with artificial feathers capable of both symmetrical and asymmetrical morphing and obtained improved low-speed maneuverability, turn radius, and high-speed flight performance. They also compared computational simulations with experimental

wind-tunnel tests. Their design was providing lift coefficient increment up to 32% and minimum drag coefficient reduction up to 40%.

Jo et al. [19] proposed a camber-morphing airfoil design applied on an already existing RQ-7a Shadow UAV wing which resulted in enhanced range and endurance. They were aerodynamically investigated a number of NACA airfoils on ANSYS Fluent at various angles of attack. They determined the configurations that provide same lift force with the original wing design using flap deflection, and consequently obtained up to 60% improvement in range and endurance.

In summary of the related works, while conventional fixed-wing designs aim to meet the requirements of a specific scenario, a morphing design has the potential to be capable of achieving multi-purposes simultaneously, such as aerodynamics and control. Therefore, this paper proposes an investigation of a multidisciplinary improvement potential on both aerodynamic and autonomous flight performances.

3. Materials and Methods

3.1. Morphing Design and Effects on Flight Dynamics

This section briefly presents the main wing of an aircraft to be redesigned and the philosophy behind the concerned morphing idea. The effects of such an application on aircraft longitudinal flight dynamics are described together with brief fundamental knowledge of dynamic modeling. To obtain aerodynamic variables of the model, a computational methodology is explained and grid independence analysis is caried out.

3.1.1. Morphing Wing Design

ZANKA-I is a fixed-wing unmanned aerial vehicle with a 1300 mm wingspan manufactured at Erciyes University, Türkiye [33]. Within the scope of this study, the main wing of the vehicle is redesigned having the ability to change its shape via tapering. The wing is divided into morphing and rectangular planforms where chord lengths of the sections are designated as c_1, c_2, and c_3, as shown in Figure 1. The application is aimed wing planform to evolve a semi-tapered design by means of tip chord length (c_3) alteration, where the wing root section has a rectangular planform same as the former base model.

In order to have an aerodynamically efficient redesigning process, wing area of the base design is conserved not to have a loss in lift force generation due to a wing area decrement. In that case, alteration in taper ratio naturally results in a change in wingspan. In the morphing scenario, the only chord length to be altered is c_3, where c_1 and c_2 is constantly 250 mm. The morphing wingtip section is designed to have a taper ratio (λ_2) varying between 1 and 0.2, and the wingtip chord length at every tapering design can be obtained

Figure 1
ZANKA-I main wing design morphing scenario divided into planform sections
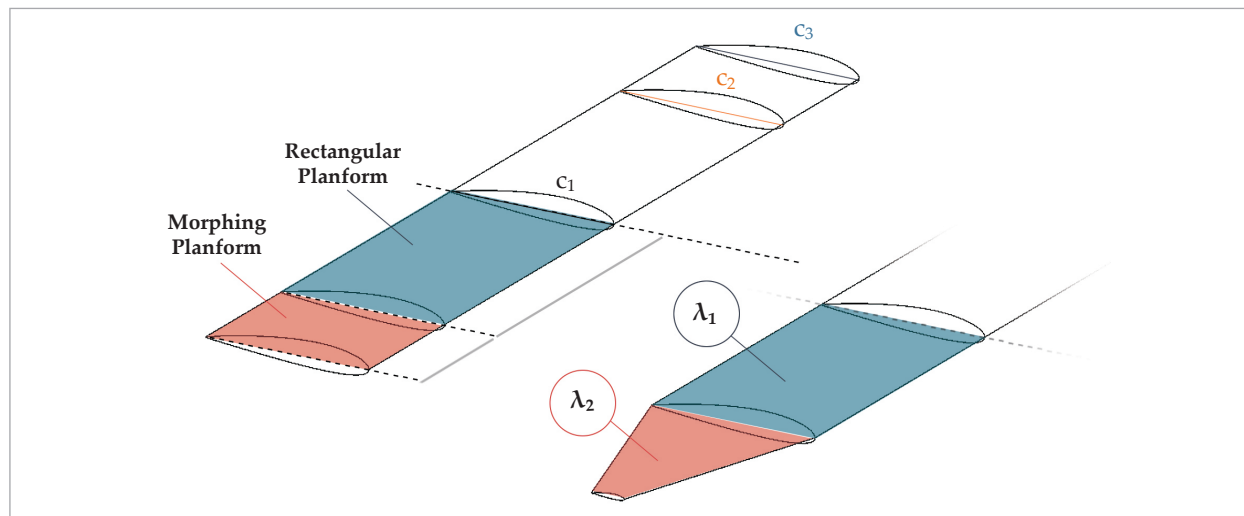
from Equation (1). Wing taper ratio (λ) can be obtained from Equation (2), where the taper ratio of the rectangular planform is constant (λ_1=1).

$$c_3 = c_2\lambda_2 \tag{1}$$

$$\lambda = \frac{0,45\lambda_1 + 0,2*\lambda_2}{0,65}. \tag{2}$$

3.1.2. Aircraft Dynamic Modeling

The dynamic model of an aircraft defines the inflight dynamic characteristics of the vehicle such as stability or controllability with the help of a set of mathematical equations. Compared with conventional designs, morphing UAVs exhibit stronger, nonlinear, time-varying and highly coupled dynamic characteristics, especially in the case of active morphing. Therefore, constructing a proper and accurate dynamic model has a key role in determination of flight performance and characteristics. The methods for dynamic modeling of a morphing vehicle could be categorized as parametric modeling, multi-body modeling, and flexible body modeling [24]. The common parametric modeling method describes the nonlinear time-varying characteristics of a system and has two types as the State-space model and the input-output model. In this study, the longitudinal dynamic model of the morphing aircraft is constructed via the state-space parametric modeling and is transformed into a linear structure by parameterization. The model consists of linearized longitudinal aircraft equations of motion in terms of force, moment, and kinematic equations of motion with state variable representation as sets of first-order differential equations [31]. In Equation (3) the abbreviated, and in Equation (4), the expanded parametric state-space form of longitudinal equations are given, where x_s and u_s are state and control vectors, and A and B are stability and control matrices, respectively. The B_{gust} matrice is an additional element related to von Karman's spectral form of random continuous turbulence applied with the aim of modeling winds, gusts, and turbulence created by atmospheric air movements. With respect to aircraft frame of reference, u, v and w are linear velocities in m/s, p, q and r, are angular velocities in rad/s and θ, ϕ, and β are pitch, roll, and sideslip angles in radians, respectively. Further and extended information of the model and stability and control derivatives can be achieved from [31, 33].

Stability and control derivatives in the equation are related with coefficients derived from aerodynamic and stability derivatives, mass, and inertia characteristics of the vehicle. For instance, the derivative Zw is the z-axis force derivative related with linear velocity w and depends on unitless aerodynamic parameters $C_{L\alpha}$ and C_{D0} as stated in Equation (5), where dynamic pressure (Q) in Pascal, wing area (S) in meters, maximum takeoff weight (m) in kilograms, and airspeed (u_0) in meters per second.

$$\dot{x} = Ax_s + Bu_s + B_{gust} \tag{3}$$

$$\begin{bmatrix} \Delta\dot{u} \\ \Delta\dot{w} \\ \Delta\dot{q} \\ \Delta\dot{\theta} \end{bmatrix} = \begin{bmatrix} X_u & X_w & 0 & -g \\ Z_u & Z_w & u_0 & 0 \\ M_u + M_{\dot{w}}Z_w & M_w + M_{\dot{w}}Z_w & M_q + M_{\dot{w}}u_0 & 0 \\ 0 & 0 & 0 & 0 \end{bmatrix} \begin{bmatrix} \Delta u \\ \Delta w \\ \Delta q \\ \Delta\theta \end{bmatrix}$$

$$+ \begin{bmatrix} X_{\delta_T} & X_{\delta_e} \\ Z_{\delta_T} & Z_{\delta_e} \\ M_{\delta_T} + M_{\dot{w}}Z_{\delta_T} & M_{\delta_e} + M_{\dot{w}}Z_{\delta_e} \\ 0 & 0 \end{bmatrix} \begin{bmatrix} \Delta\delta_T \\ \Delta\delta_e \end{bmatrix} + \tag{4}$$

$$+ \begin{bmatrix} -X_u & -X_w & 0 \\ -Z_u & -Z_w & 0 \\ -M_u & -M_w & -M_q \\ 0 & 0 & 0 \end{bmatrix} \begin{bmatrix} u_g \\ w_g \\ q_g \end{bmatrix}$$

$$Z_w = \frac{-(C_{L_\alpha} + C_{D_0})QS}{mu_0}. \tag{5}$$

In Equation (6), another moment derivative M_w is related with linear velocity w is given and simply depends on both $C_{m\alpha}$ and y-axis area moment of inertia (I_y), where c is the mean aerodynamic chord length (MAC) of the wing in meters.

$$M_w = C_{m_\alpha} \frac{QS\bar{c}}{u_0 I_y}. \tag{6}$$

Similarly to the mentioned examples, observation of the flight dynamics of a morphing aircraft requires the investigation of the effects of morphing and effective variables to the full extent.

3.1.3. Effects of Morphing on UAV Flight Dynamics

The redesign of a fixed-wing aerial vehicle with morphing ability results in geometrical, aerodynamical, and inertial alterations, and impacts on vehicle dynamics,

which are required to be investigated. In this regard, the base and morphed ZANKA-I UAV main wing designs at various wingtip taper ratios are presented in Figure 2, where chord lengths at determined spanwise locations are identified similar with Figure 1.

Figure 2

The base and morphed wing designs with various wingtip taper ratios
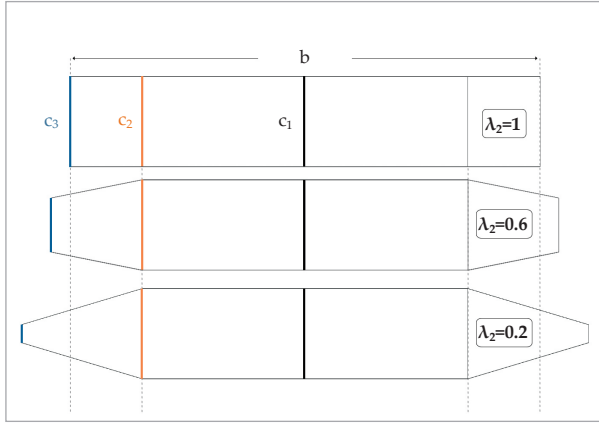
Since the wing area is preserved as constant, the decrease in wingtip taper ratio simply leads to an increased wing span (b), aspect ratio (AR) and sweep angle (Λ), while wing taper ratio, mean aerodynamic chord length, and wingtip chord length are decreased. AR and MAC are expressed in terms of wing span, wing area, and chord lengths c_1, c_2 and c_3 as given in Equation (7) and Equation (8). The variation in some geometrical parameters of the morphing wing with wingtip taper ratios ranging from 1 to 0.2 is summarized with 0.2 intervals in Table 1.

$$AR = \frac{b^2}{S} \tag{7}$$

$$MAC = \left(\left(\frac{c_1 + c_2}{2} \right) * 0.45 + \left(\frac{c_2 + c_3}{2} \right) * 0.2 \right) / 0.65 . \tag{8}$$

The moment of inertia indicates the resistance to rotation about related axis of the aerial vehicle. The inertia of the aircraft tensor associated with body-fixed reference frame is given in Equation (9), where I_{xx}, I_{yy} and I_{zz} are the terms with respect to x, y and z axis [49]. Moreover, I_{xy}, I_{xz} and I_{yz} are products of inertia related to xy, xz and yz planes, respectively.

Table 1

Geometric parameters varying with wingtip taper ratio

λ_2	1.0	0.8	0.6	0.4	0.2
λ	1.0	0.938	0.876	0.815	0.753
b [mm]	1300	1344	1400	1471	1567
AR	5.2	5.562	6.031	6.662	7.552
MAC [mm]	250	243	236	230	226
Λ [deg]	0	1.065	2.044	2.918	3.652
c_3 [mm]	250	200	150	100	50

$$\overline{I} = \begin{bmatrix} I_{xx} & -I_{xy} & -I_{xz} \\ -I_{xy} & I_{yy} & -I_{yz} \\ -I_{xz} & -I_{yz} & I_{zz} \end{bmatrix} . \tag{9}$$

As the design of the aircraft is assumed to have xz plane of symmetry, I_{xy} and I_{yz} equals to zero. Thus, the values of remaining inertial terms and variations with wingtip taper ratio are estimated from full-scale computer-aided design model of the vehicle and calculated by using the parallel-axis theorem and summarized in Table 2.

Table 2

Inertial parameters varying with wingtip taper ratio

λ_2	1.0	0.8	0.6	0.4	0.2
I_{xx} [kgm^2]	0.0987	0.0960	0.0930	0.0900	0.0873
I_{yy} [kgm^2]	0.1421	0.1351	0.1312	0.1295	0.1293
I_{zz} [kgm^2]	0.2297	0.2232	0.2163	0.2094	0.2032
I_{xz} [kgm^2]	0.0127	0.0118	0.0105	0.0095	0.0089

An alteration is also arisen in terms of aerodynamic parameters (i.e. reference drag and lift coefficients, C_{L0} and C_{D0}, lift and drag curve slopes, $C_{L\alpha}$ and $C_{D\alpha}$, Oswald efficiency factor (e), of the wing due to the morphological differentiation, and directly affects stability and control derivatives of the aircraft dynamic model. The panel methods model wing surfaces by panels and singularities, and are proper computation-

al options for the investigation of such a conceptual morphing design idea [29]. XFLR5 is a general public licensed powerful tool capable of analyzing aerodynamic parameters using the 3D-panel method and Dirichlet boundary conditions integrated with viscous effects [45]. 3D-panel method estimates the flow characteristics by closing entire volume of the wing with quad-shaped flat panel elements, where source and doublet strengths are defined uniformly. In such a finite-element assessment, grid independence analysis is conducted to have optimal computational time and accuracy, and carried out in case of a steady level flight at 60 km/h airspeed and sea-level conditions with number of panels up to 1×10^4. The results given in Figure 3 indicates that approximately 5×10^3 panels are adequate for admissibly accurate results in the cruising flight. The distribution of generated ad-

equate number of 3D-panels on semi-tapered main wing design with λ_2 value of 0.2 is given in Figure 4.

Figure 4
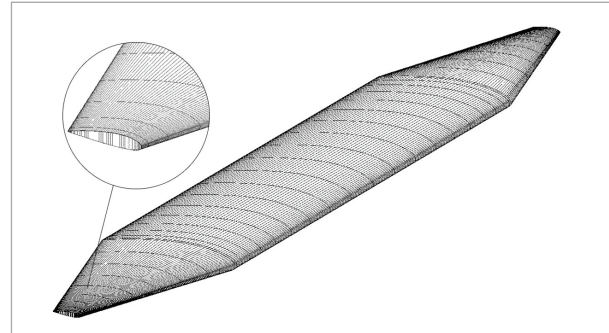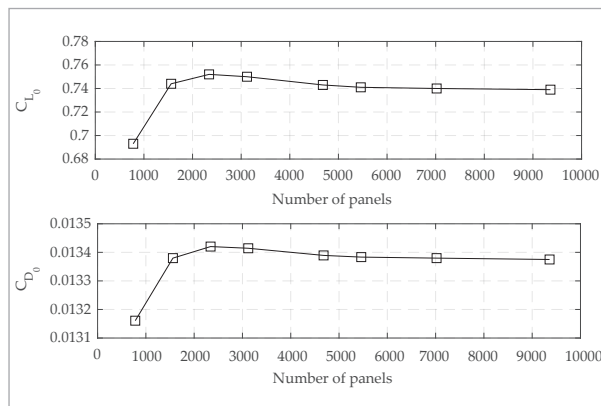Distribution of generated panels on semi-tapered design with λ_2=0.2
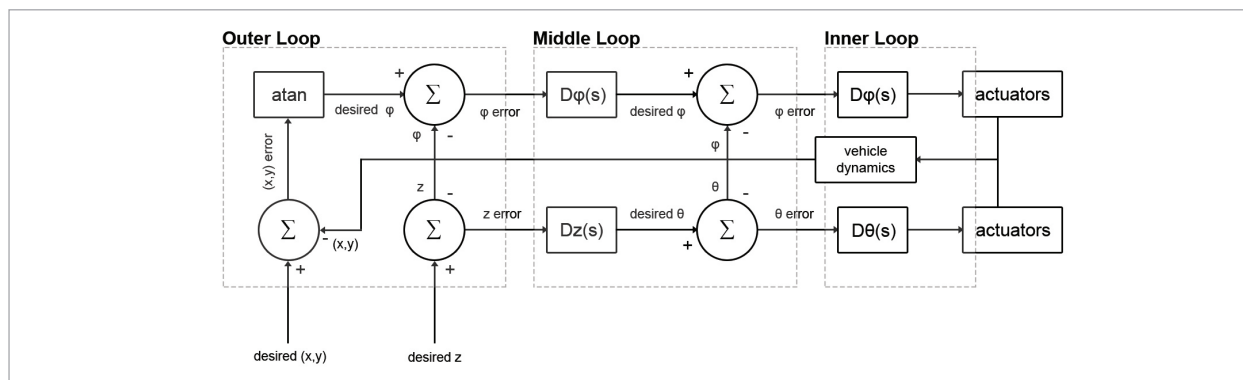

3.2. Control System Design

The control system is applied in a traditional form composed of outer, middle and inner layers arranged as given in Figure 5. The inner layer is responsible for roll (φ) and pitch (θ) attitudes while heading and altitude stabilization is carried out by the middle layer and x-y position tracking by the outer layer [17]. The autonomous flight control is provided by six PID controllers for longitudinal and lateral attitudes, due to the design simplicity and easy adjustability of PID algorithm. Correspondingly, autonomous flight performance is dramatically affected by the proportional (k_P), integral (k_I), and derivative (k_D) coefficients of the controllers and should be properly tuned during or pre-flight.

Figure 3
Reference lift and drag coefficient results changing with generated number of panels

Figure 5
Hierarchically structured control system design

3.3. Simultaneous Design Approach

The simultaneous design of a morphing aerial vehicle and flight control system leads to a need for a number of parameters to be determined. Within the context of this study, our design problem has variables of longitudinal PID controller coefficients to be tuned and wingtip taper ratio to be estimated with the aim of maximizing LAFP. As solving such a complex problem with analytical methods is almost unfeasible, a gradient-free stochastic optimization algorithm called SPSA is conducted to provide the desired solution. Moreover, the k-NN machine learning algorithm is used in the estimation of dynamic model variables to expand data for obtaining more sensitive results in optimization.

3.3.1. Simultaneous Perturbation Stochastic Approximation

The stochastic approximation (SA) is a proper recursive method for finding the roots of mathematical equations in the presence of noisy measurements [29]. In the case of noisy loss function data, there are outperforming gradient-free models of SA such as Simultaneous Perturbation SA or Random-direction SA (RDSA) that come to the fore rather than finite-difference approaches to reach the global minimum value [28]. SPSA is well-known to be successfully applied in many aerospace applications such as flight path planning [20, 26] and aerodynamic shape and control system designs [40, 46, 47]. The algorithm is exhibited to estimate the gradient of a multivariate differentiable cost function. The main advantage is to have too few numbers of recursion for cost function evaluation that is mentioned as the most expensive part of an optimization problem. Further information and theoretical basis of the method might be reached from [37, 38].

In our problem, cost function is constituted from sum of longitudinal reference trajectory tracking qualities of rise time, settling time and maximum overshoot with the aim of obtaining best LAFP. The variables to be estimated are defined as the wingtip taper ratio and PID coefficients of the longitudinal controller which greatly affects the dynamic model parameters of the vehicle. Cost-index (J_{long}) is presented in Equation (10) in terms of rise time (T_{rt}), settling time (T_{st}) and maximum overshoot (*OS*).

$$J_{long} = (T_{rt} + T_{st} + OS)_{longitudinal} . \tag{10}$$

The objective of the algorithm is to minimize the given cost-index from its initial value. The cycle of the algorithm ends when there is a nonsignificant change in the cost function in several consecutive iterations or when the defined maximum number of iterations is reached which is defined as 10 in our case with respect to previous studies. Improvement in the total cost-index of the LAFP might be obtained from Equation (11) in percentage for each iteration.

$$\%J_{long_i} = \frac{100\left(J_{long_i} - J_{long_0}\right)}{J_{long_0}} . \tag{11}$$

3.3.2. k-Nearest Neighbors (k-NN) Machine Learning Algorithm

The k-NN algorithm is a non-parametric supervised method that serves for regression or classification to provide predictions using the proximity of a group of individual data points [39]. The term, k, denotes the number of neighbors nearest to the test object to be considered in the training data set. In the estimation of any variable, it should be chosen appropriately to adjust the performance of the algorithm [51]. In k-NN regression using the Euclidean distance metric, the distance between the sample and the predicted value might be obtained from Equation (12), where x denotes the sample vector and n is the number of training data [23]. The k samples having minimum Euclidean distance for the sample vector x_i are picked and an average of their y_i is regarded as the predicted value to find the relevant value on the regression curve.

$$d(x, y) = \sqrt{\sum_{i=1}^{n} (x_i - y_i)^2} . \tag{12}$$

In our morphing design problem, the variables of the aircraft dynamic model (i.e. aerodynamic coefficients, stability and control derivatives, moments of inertia terms, etc.) are investigated depending on wingtip taper ratio values between 1 and 0.2 with a 0.05 interval, which results in 17 different morphing scenarios to be used as the training data. For the purpose of having more comprehensive and accurate optimization results, the predictions of the expanded number of tapering variations are obtained within the constraints of the design problem by the implementation of the k-NN regression algorithm.

4. Results and Discussion

4.1. Aerodynamic Effects of Morphing

Aerodynamic analyses of the morphing wing carried out on XFLR5 program using 3D panel method with 5×10^3 structured panels enclosing the wing surface. Each wing model generated with a wingtip taper ratio varying from 1 to 0.2 with a 0.05 interval, and a summary of aerodynamic results are given in Table 3.

Table 3
Aerodynamic parameters varying with wingtip taper ratio

| λ_2	1.0	0.8	0.6	0.4	0.2
C_{L0}	0.6494	0.6694	0.6921	0.7173	0.7429
C_{D0}	0.0132	0.0128	0.0120	0.0126	0.0133
L/D	49.09	52.04	57.21	56.53	55.48
$C_{L\alpha}$	4.8242	4.9949	5.1923	5.4178	5.6522
$C_{D\alpha}$	0.1000	0.0999	0.0992	0.0997	0.0953
e	1.0130	1.0210	1.0301	1.0362	1.0322

The wingtip taper ratio decrement is clearly seen to raise Oswald efficiency factor to increase expectedly due to a higher aspect ratio planform and providing better lift distribution than rectangular planform. Similarly, reduction in lift-induced drag in virtue of diminished wingtip vortices formations on tapered planform resulted in total drag reduction [15]. However, excessive tapered planforms led to remarkable adverse effects to be considered in terms of drag-related parameters. While the drag curve slope is found to decrease polynomially, the lift curve slope is responded inversely proportional to the wingtip taper ratio. Moreover, the reference lift coefficient is shown a tendency to increase for the increasing amount of tapering for the whole interval. Nevertheless, the reference drag coefficient is found to show an imbalanced tendency composed of incremental and decremental sections within the interval. Consequently, the obtained tendencies of aerodynamic parameters are found in good agreement with similar investigations in the literature [2, 30]. The detailed results of geometric, aerodynamic and inertial parameters are given in Figures A1-A3, respectively.

The simultaneous lift and mostly drag coefficient decrement ensured an improvement in the lift-to-drag ratio, which is earlier mentioned as aerodynamic performance enhancement. As the base design has a rectangular-shaped planform, every tapered variation of the design is found to have superior aerodynamic performance as desired and given in Figure 6. While maximum performance improvements obtained approximately at medium tapered designs, excessively tapered planforms led to a bit of aerodynamic performance losses.

Figure 6
Aerodynamic performance with respect to wingtip taper ratio
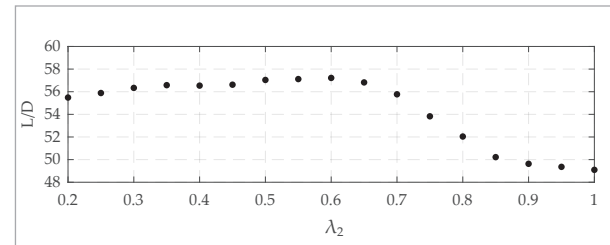
4.2. Simultaneous Design Approach

The examined geometrical, aerodynamical, and inertial alterations due to the morphing application are presented in the previous section and almost all of the emphasized terms are evidently seen to have a nonlinear relationship with the wingtip taper ratio as clearly presented in Appendix A. These parameters are also well-known to affect aircraft dynamic model substantially in terms of stability and control derivatives. As a part of the simultaneous design approach established in this paper, it is supposed to estimate the most proper wingtip taper ratio together with PID controller coefficients in an effort to obtain maximum LAFP. In this regard, for solving the optimization problem including such complex relationship, the SPSA optimization algorithm is applied.

The geometrical, aerodynamic, and inertial data obtained with specific increments formerly are used as training data and expanded via the k-NN regression in the MATLAB environment. The k value is selected as 3 by means of trial-error method on the training data for providing the most accurate predictions during optimization. The regression code is linked to the aircraft dynamic model to constitute the model for every wingtip taper ratio between 1 to 0.2. The SPSA code is regulated to optimize the related parameters to successfully track a longitudinal trajectory of a 5-degree

pitch angle. Initial values of longitudinal PID coefficients and wingtip taper ratio are determined as 50, 5, 50, and 1, respectively.

The results of SPSA optimization in terms of longitudinal PID coefficients, wingtip taper ratio, longitudinal cost-index and lift-to-drag ratio are summarized in Table 4. Aerodynamic performance is increased approximately by 14.32%, while a decrement is obtained in the longitudinal cost-index, which stands for improvement in trajectory tracking quality by 41.7% with regard to the initial design.

Table 4

Initial and final values of optimized parameters and performance metrics

	Initial value	Final value
k_P	50	29.98
k_I	5	7.25
k_D	50	74.97
λ_2	1	0.2746
J_{long}	0.61398	0.35793
L/D	49.09	56.12

In Figure 7, the change in longitudinal PID coefficients and wingtip taper ratio during ten iterations of optimization process is presented, where the first iterations are denoted as "0". It is evident that the SPSA algorithm is already converged in a few numbers of iterations for both variables to be estimated. The optimization algorithm tended to decrease the proportional and integral coefficients while increasing the differential coefficient with respect to their initial values. The increment in the differential coefficient stirred up a substantial decrease in maximum overshoot and dropped integral coefficient served for the decreased rise time as expected.

The cost-index value and accordingly improvement in percentage are also converged within the few numbers of iterations as shown in Figure 8. The obtained

Figure 7

The convergence of longitudinal PID coefficients and wingtip taper ratio with respect to iteration index
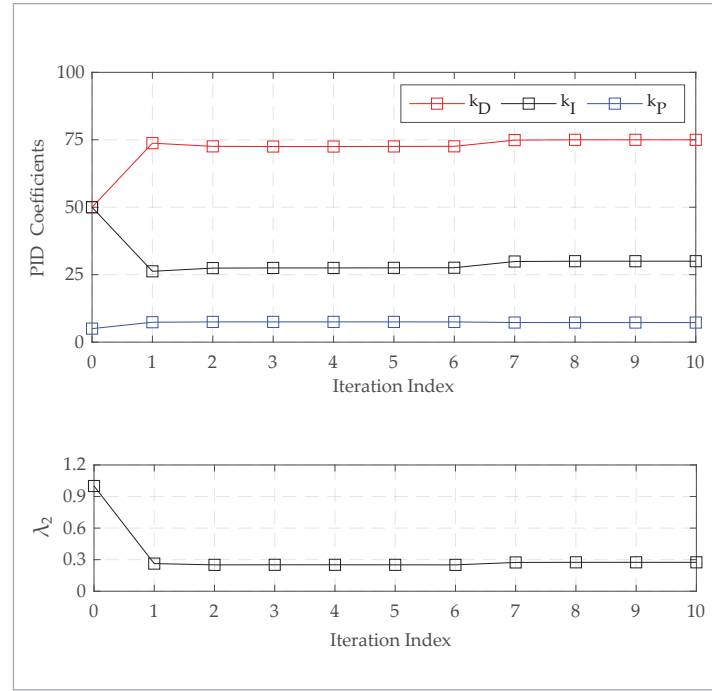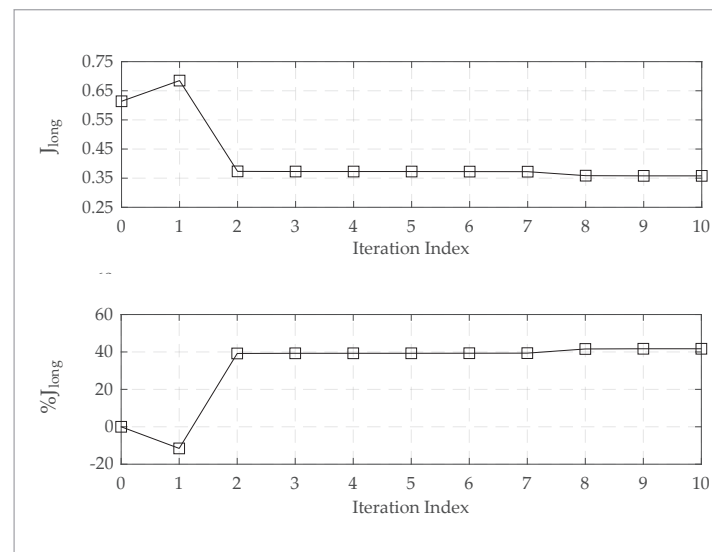

Figure 8

The percentage improvement in longitudinal cost-index with respect to iteration index

decrement in cost-index implies improvement in the longitudinal trajectory tracking qualities which is defined as the sum of maximum overshoot, rise time, and settling time. Consequently, the main wing design is optimized and the geometrical parameters of the new morphing wing are given in Table 5.

Table 5
Initial and final values of optimized parameters and performance metrics

	Initial value	Final value
MAC [mm]	250	228
b [mm]	1300	1528
λ	1	0.77
AR	5.2	7.182
c_3 [mm]	250	68.75
Λ [deg]	0	3.39

The wing span is extended by 17.3%, the wing aspect ratio is increased by 38.1%, and the planform is tapered by 23% from the initial design via the SPSA algorithm. Wingtip chord length, c_3, is also substantially decreased that led the un-swept rectangular wing planform to transform into a semi-tapered design with a positive sweep angle.

4.3. Flight Simulations

The ZANKA-I UAV is redesigned with morphing wing and optimized in previous section. The closed-loop responses of the new design will be discussed in this section with flight simulations. The dynamic model of the aircraft is used in form of the parametrical state-space model integrated with gust disturbance vectors as given previously in Equation (4). The vehicle is supposed to track the 5-degrees pitch angle (θ_{ref}) autonomously by using its hierarchical structured control system composed of three PID controllers. In Figure 9, block-diagram of the simulation on MATLAB/Simulink environment is given. During the simulations, elevator deflection is constrained from -30 to 30 degrees.

As a result, closed-loop responses within 60 seconds in terms of elevator deflection (δ_e), linear velocities along x and z axes, and roll rate (q) within 60 seconds

Figure 9
Longitudinal autonomous flight simulation block-diagram on MATLAB/Simulink
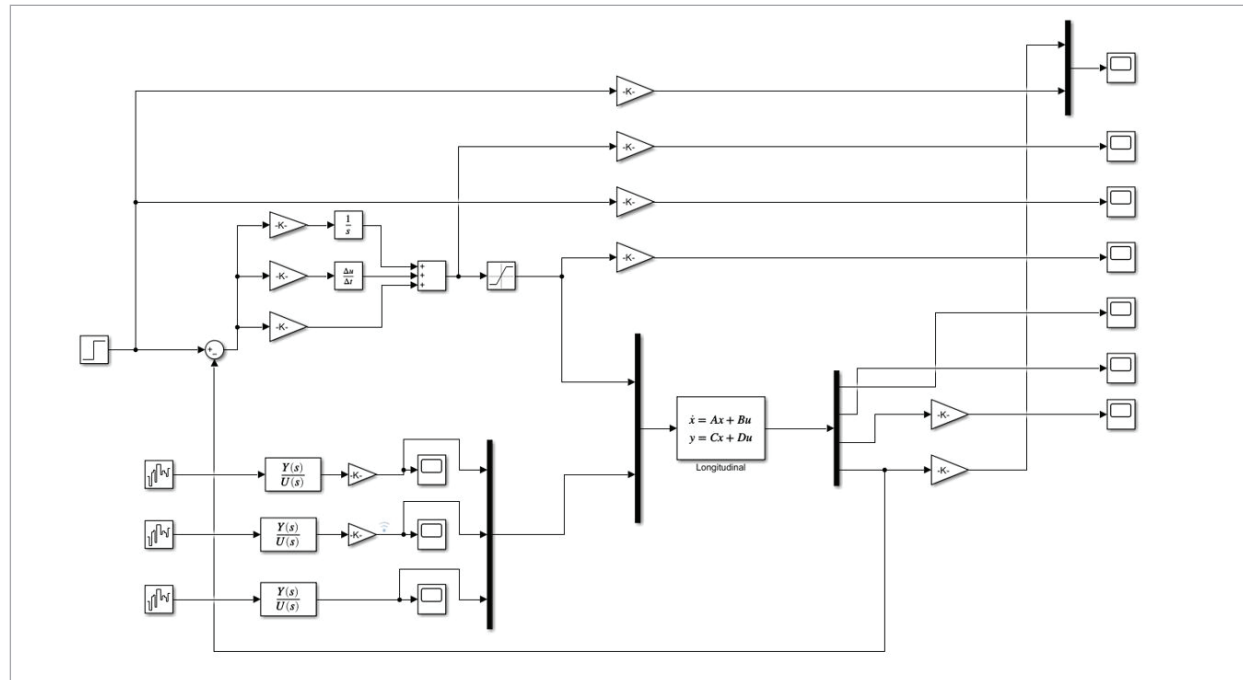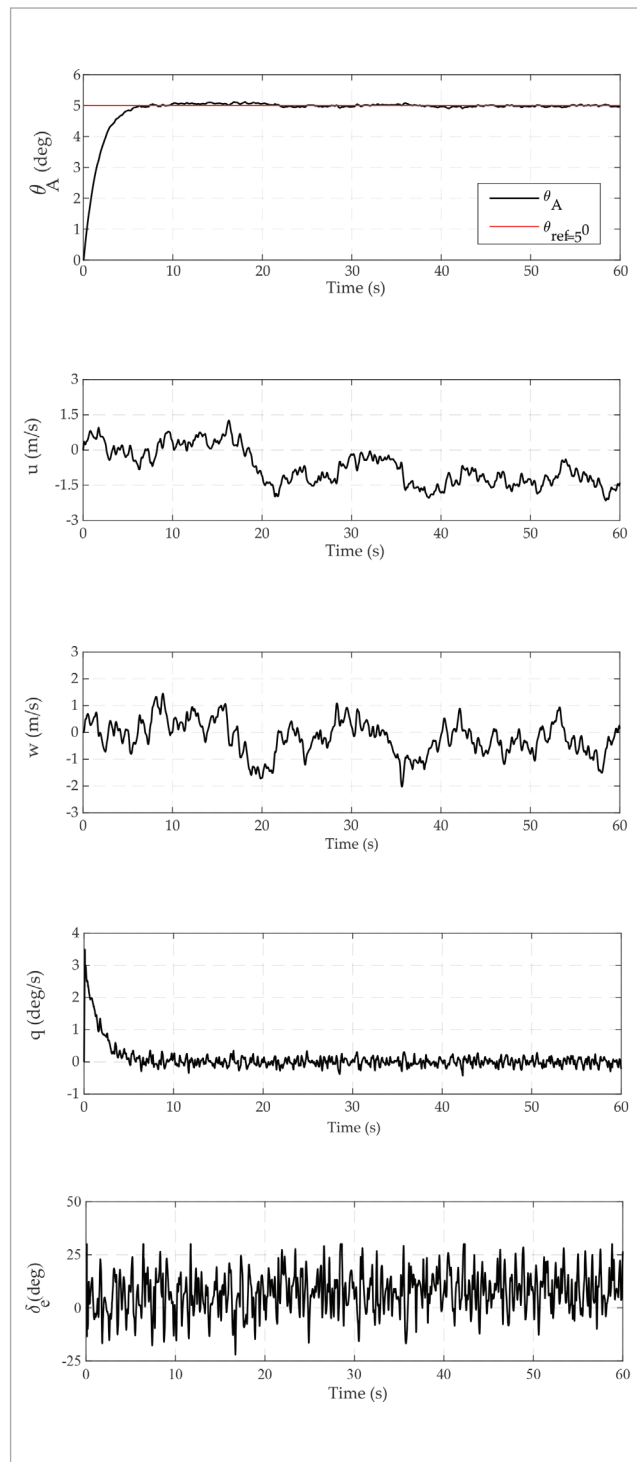
Figure 10

Closed-loop responses of longitudinal motion

are given in Figure 10. The autonomous flight performance is clearly seen to be successful even under pure turbulence and desired trajectory tracking is obtained, where any catastrophic behaviors are not observed during the overall duration.

5. Conclusions

Simultaneous aircraft design methodology comprising a novel morphing wing and control system design was proposed in this study. Within the scope of the study, the rectangular main wing of a fixed-wing UAV was renovated with an innovative morphing design capable of tapering from a defined spanwise distance up to wingtips. To obtain the morphing aircraft dynamic model, aerodynamic, geometrical, and inertial investigations were carried out within the constraints of the morphing scenario at limited intervals. Additionally, the corresponding limited data were extended via the k-NN machine learning algorithm as it is not feasible to investigate the infinite number of morphing scenarios for optimization. The algorithm served successfully as a powerful tool for such applications and the performance of various algorithms could be investigated as a future study.

The hierarchically structured longitudinal control system with three PID controllers was presented, and the PID coefficients were defined as the variables to be optimized together with the wingtip taper ratio as the proposed simultaneous design approach demands. Since every morphing scenario within determined constraints was found to result in aerodynamically improved performance, the optimization problem is focused on the maximization of LAFP, and the SPSA optimization algorithm was conducted.

In conclusion, the simultaneous morphing wing and control system design idea incorporated with SPSA optimization provided a considerable improvement in aerodynamic and longitudinal autonomous flight performances than the initial condition. The optimization method found to be very useful for such a complex problem and resulted in a number of iterations. The aerodynamic performance standing for the lift-to-drag ratio

was increased by 14.32%, while autonomous flight performance standing for the sum of longitudinal trajectory tracking qualities of maximum overshoot, rise time, and settling time is increased by 41.7%.

Longitudinal and lateral trajectory tracking tests of the morphing design were performed with flight simulations for reference tracking attitude of 5-degree pitch angle. Satisfactory closed-loop responses were obtained without any catastrophic oscillations while reference trajectory was found to be tracked successfully even under the existence of pure turbulence.
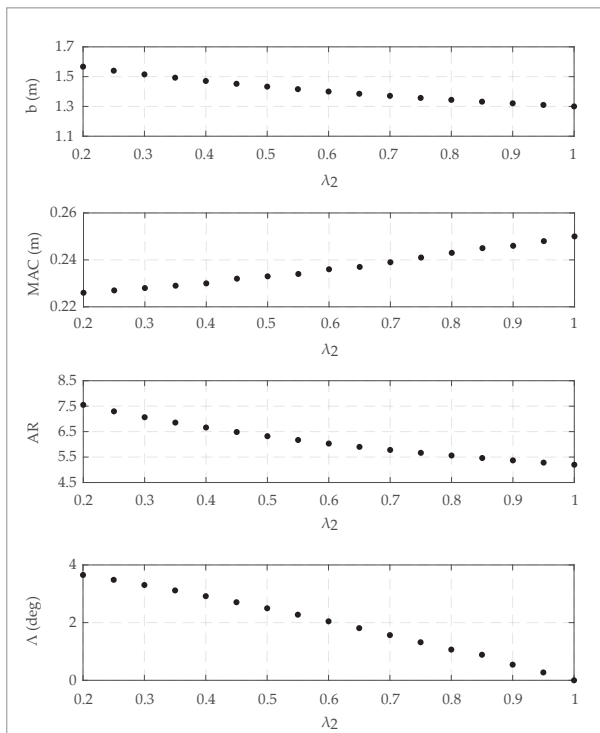
From a trajectory tracking point of view, this study is particularly focused on longitudinal motion, and could be extended to lateral motion or a combination of both as future work.

Appendix A

The alterations in geometrical parameters of the morphing wing are given in Figure A1. The decrease

in wingtip taper ratio simply leads to an increase in wingspan, aspect ratio and sweep angle while, a decrease in the mean aerodynamic chord. Correspondingly, the results of aerodynamic investigations of the morphing wing are presented in Figure A2, and inertial alterations in Figure A3.

Figure A1

Geometric variables changing with wingtip taper ratio

Figure A2

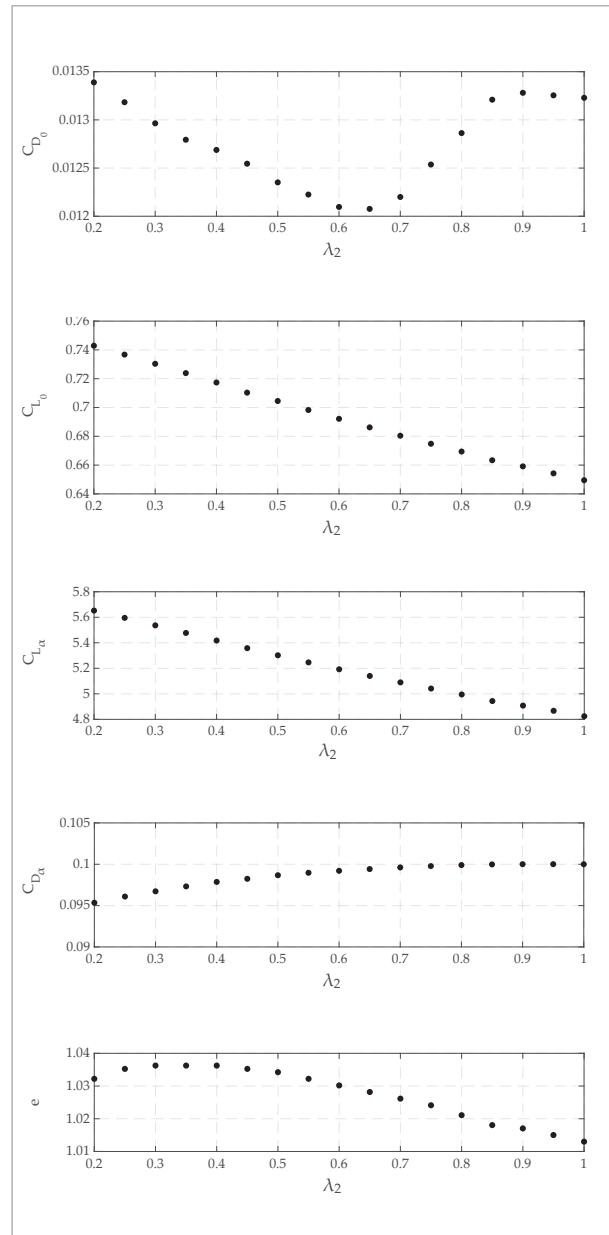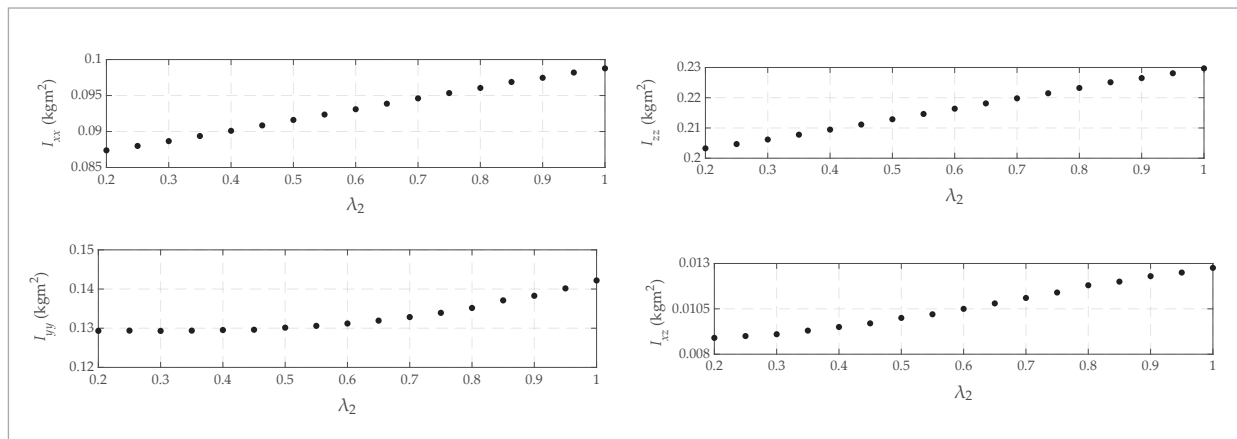Aerodynamic variables changing with wingtip taper ratio

Figure A3
Inertial variables changing with wingtip taper ratio

References

1. Abdulrahim, M., Lind, R. Flight Testing and Response Characteristics of a Variable Gull-Wing Morphing Aircraft. In Proceedings of the AIAA Guidance, Navigation, and Control Conference and Exhibit, Providence, Rhode Island, 2004. https://doi.org/10.2514/6.2004-5113

2. Ananda, G. K., Sukumar, P. P., Selig, M. S. Measured Aerodynamic Characteristics of Wings at Low Reynolds numbers. Aerospace Science and Technology, 2015, 42, 392-406. https://doi.org/10.1016/j.ast.2014.11.016

3. Barbarino, S., Bilgen, O., Ajaj, R. M., Friswell, M. I., Inman, D. J. A Review of Morphing Aircraft. Journal of Intelligent Material Systems and Structures, 2011, 22(9), 823-877. https://doi.org/10.1177/1045389X11414084

4. Binbin, Y., Yong, L., Pei, D., Shuangxi, L. Aerodynamic Analysis, Dynamic Modeling, and Control of a Morphing Aircraft. Journal of Aerospace Engineering, 2019, 32(5), 04019058. https://doi.org/10.1061/(ASCE) AS.1943-5525.0001047

5. Bons, N. P., He, X., Mader, C. A., Martins, J. R. R. A. Multimodality in Aerodynamic Wing Design Optimization. AIAA Journal, 2019, 57(3), 1003-1018. https://doi.org/10.2514/1.J057294

6. Bronz, M., Tal, E., Favalli, F., Karaman, S. Mission-Oriented Additive Manufacturing of Modular Mini-UAVs. In Proceedings of the AIAA Scitech Forum, Orlando, FL, 6-10 January 2020. https://doi.org/10.2514/6.2020-0064

7. Gandolfo, D. C., Salinas, Brandão, A. S., Toibero, J. M. Path Following for Unmanned Helicopter: An Approach on Energy Autonomy Improvement. Information Technology and Control, 2016, 45(1), 86-98. https://doi.org/10.5755/j01.itc.45.1.12413

8. Di Luca, M., Mintchev, S., Heitz, G., Noca, F., Floreano, D. Bioinspired Morphing Wings for Extended Flight Envelope and Roll Control of Small Drones. Interface Focus 2017, 7(1), 20160092. https://doi.org/10.1098/rsfs.2016.0092

9. Dussart, G., Portapas, V., Pontillo, A., Lone M. Flight Dynamic Modelling and Simulation of Large Flexible Aircraft. In Flight Physics: Models, Techniques and Technologies, Volkov, K., Eds., InTech, Rijeka, Croatia, 2018, 49-72. https://doi.org/10.5772/intechopen.71050

10. Elelwi, M., Kuitche, M., Botez, R., Dao, T. Comparison and Analyses of a Variable Span-morphing of the Tapered Wing with a Varying Sweep Angle. The Aeronautical Journal, 2020, 124(1278), 1146-1169. https://doi.org/10.1017/aer.2020.19

11. Emad, D., Mohamed, A., Fanni, M. Modeling and Flight Control of Small UAV with Active Morphing Wings. Journal of Intelligent & Robotic Systems, 2022, 106, 42. https://doi.org/10.1007/s10846-022-01740-y

12. Falcão, L., Gomes, A., Suleman, A. Aero-structural Design Optimization of a Morphing Wingtip. Journal of Intelligent Material Systems and Structures, 2011, 22(10), 1113-1124. https://doi.org/10.1177/1045389X11417652

13. Franco, A., Alberto, S., Alex, Z., Giuseppe, G., Daniele, Z., Yannick, B.T., Marianna B. Experimental Evaluation of the Aerodynamic Performance of a Large-Scale High-Lift Morphing Wing. Aerospace Science and Technology, 2022, 124, 107515. https://doi.org/10.1016/j.ast.2022.107515

14. Gudmundsson, S. General Aviation Aircraft Design: Applied Methods and Procedures, 2nd ed., Elsevier Science: Butterworth-Heinemann, Cambridge MA, USA, 2021, 322-412.

15. Güzelbey, İ.H., Eraslan, Y., Doğru, M. H. Effects of Taper Ratio on Aircraft Wing Aerodynamic Parameters: A Comperative Study. European Mechanical Science, 2019, 3(1), 18-23. https://doi.org/10.26701/ems.487516

16. Hintz, C., Torno, C., Carrillo, L. R. G. Design and Dynamic Modeling of a Rotary Wing Aircraft With Morphing Capabilities. In Proceedings of the International Conference on Unmanned Aircraft Systems (ICUAS), Orlando, FL, USA, 27-30 May 2014. https://doi.org/10.1109/ICUAS.2014.6842290

17. Jang, J. S., Liccardo, D. Automation of Small UAVs using a Low Cost Mems Sensor and Embedded Computing Platform. In Proceedings of the 25th Digital Avionics Systems Conference, Portland, OR, USA, 15-19 October 2006. https://doi.org/10.1109/DASC.2006.313772

18. Jasa, J. P., Hwang, J. T., Martins, J. R. R. A. Design and Trajectory Optimization of a Morphing Wing Aircraft. In Proceedings of the AIAA/ASCE/AHS/ASC Structures, Structural Dynamics, and Materials Conference, Kissimmee, Florida, 8-12 January 2018. https://doi.org/10.2514/6.2018-1382

19. Jo, B. W., Majid, T. Enhanced Range and Endurance Evaluation of a Camber Morphing Wing Aircraft. Biomimetics, 2023, 8(1), 34. https://doi.org/10.3390/biomimetics8010034

20. Konstantin, A., Vladimir, M. Using of the SPSA Method to Improve the Accuracy of UAV Following a Given Route Under the Action of Wind Loads. Cybernetics and Physics, 2021, 10(4), 224-230. https://doi.org/10.35470/2226-4116-2021-10-4-224-230

21. Kose, O., Oktay, T. Hexarotor Yaw Flight Control with SPSA, PID Algorithm and Morphing. International Journal of Intelligent Systems and Applications in Engineering, 2022, 10(2), 216-221.

22. Kose, O., Oktay, T. Simultaneous Quadrotor Autopilot System and Collective Morphing System Design. Aircraft Engineering and Aerospace Technology, 2020, 92(7), 1093-1100. https://doi.org/10.1108/AEAT-01-2020-0026

23. Lin, Y., Guan, Z. The Use of Machine Learning for the Prediction of the Uniformity of the Degree of Cure of a Composite in an Autoclave. Aerospace, 2021, 8(5), 130. https://doi.org/10.3390/aerospace8050130

24. Lingling, C., Qi, L., Feng, G., Xintian, D., Yuqing, H., Yangchen, D. Design, Modeling, and Control of Morphing Aircraft: A Review. Chinese Journal of Aeronautics 2022, 35(5), 220-246. https://doi.org/10.1016/j.cja.2021.09.013

25. Liu, J., Shan, J., Hu, Y., Rong, J. Optimal Switching Control for Morphing Aircraft with Aerodynamic Uncertainty. In Proceedings of the International Conference on Control & Automation (ICCA), Singapore, 09-11 October 2020. https://doi.org/10.1109/ICCA51439.2020.9264361

26. Lu, L., Yan, X., Constantinos, A., Moshe, B. An Enhanced SPSA Algorithm for the Calibration of Dynamic Traffic Assignment Models. Transportation Research Part C: Emerging Technologies 2015, 51, 149-166. https://doi.org/10.1016/j.trc.2014.11.006

27. Majeti, R. K., Benz, S. Mission-based Optimal Morphing Parameters for Rotors with Combined Chord and Twist Morphing. Open Research Europe 2022, 1, 121. https://doi.org/10.12688/openreseurope.14060.2

28. Maryak, J. L., Chin, D. C. Global Random Optimization by Simultaneous Perturbation Stochastic Approximation. In Proceedings of the American Control Conference, Arlington, VA, USA, 25-27 June 2001. https://doi.org/10.1109/ACC.2001.945806

29. Moëns, F. A Fast Aerodynamic Model for Aircraft Multidisciplinary Design and Optimization Process. Aerospace, 2023, 10(1), 7. https://doi.org/10.3390/aerospace10010007

30. NASA Technical Reports Server (NTRS). Available online: https://ntrs.nasa.gov/citations/19930091647 (accessed on 26 February 2023)

31. Nelson, R. C. Flight Stability and Automatic Control, 2nd ed., WCB/McGraw-Hill Companies, Singapore, 1998.

32. Oktay, T., Sultan, C. Flight Control Energy Saving via Helicopter Rotor Active Morphing. Journal of Aircraft, 2014, 51(6), 1784-1804. https://doi.org/10.2514/1.C032494

33. Oktay, T., Konar, M., Onay, M., Aydin, M., Mohamed, M.A. Simultaneous Small UAV and Autopilot System Design. Aircraft Engineering and Aerospace Technology, 2016, 88(6), 818-834. https://doi.org/10.1108/AEAT-04-2015-0097

34. Rafic, M. A., Muhammed, S. P., Mohammadreza, A., Michael, I. F., Wesley, J. C. Recent Developments in the Aeroelasticity of Morphing Aircraft. Progress

in Aerospace Sciences, 2021, 120, 1-29. https://doi.org/10.1016/j.paerosci.2020.100682

35. Raymer, D. P. Aircraft Design: A Conceptual Approach, 2nd ed., American Institute of Aeronautics and Astronautics, Washington, DC, USA, 1992, 1-10.

36. Sofla, A. Y. N., Meguid, S. A., Tan, K. T., Yeo, W. K. Shape morphing of aircraft wing: Status and challenges. Materials & Design, 2010, 31(3), 1284-1292. https://doi.org/10.1016/j.matdes.2009.09.011

37. Spall, J. C. An Overview of the Simultaneous Perturbation Method for Efficient Optimization. Johns Hopkins APL Technical Digest, 1998, 19, 482-492.

38. Spall, J. C. Introduction to Stochastic Search and Optimization: Estimation, Simulation, and Control, Wiley & Sons Inc., Hoboken, New Jersey, USA, 2003. https://doi.org/10.1002/0471722138

39. Stawian, D., Daely, S. M., Heryanto, A., Afifah, N., Idris, M. Y., Budirato, R. Ransomware Detection Based On Opcode Behavior Using K-Nearest Neighbors Algorithm. Information Technology and Control, 2021, 50(3), 495-506. https://doi.org/10.5755/j01.itc.50.3.25816

40. Şahin, H., Kose, O., Oktay, T. Simultaneous Autonomous System and Powerplant Design for Morphing Quadrotors. Aircraft Engineering and Aerospace Technology 2022, 94(8), 1228-1241. https://doi.org/10.1108/AEAT-06-2021-0180

41. Ting, Y., Xiangyang, Z., Lixin, W., Junqiang, A. Flight Dynamic Modeling and Control for a Telescopic Wing Morphing Aircraft Via Asymmetric Wing Morphing. Aerospace Science and Technology, 2017, 70, 328-338. https://doi.org/10.1016/j.ast.2017.08.013

42. Valldosera, M. R., Afonso, F., Lau, F. Aerodynamic Shape Optimisation of a Camber Morphing Airfoil and Noise Estimation. Aerospace, 2022, 9(1), 43. https://doi.org/10.3390/aerospace9010043

43. Wong, A., Bil, C., Marino, M. Design and Aerodynamic Performance of a FishBAC Morphing Wing. In Proceedings of the AIAA Scitech Forum, San Diego, CA, USA, 3-7 January 2022. https://doi.org/10.2514/6.2022-1298

44. Wang, Y., Li, X., Wu, T., Yin, H. Multidisciplinary Design and Optimization of Variable Camber Wing with Non-Equal Chord. Aerospace, 2023, 10(4), 336. https://doi.org/10.3390/aerospace10040336

45. XFLR5 v6.02 Guidelines. Available online: https://sourceforge.net/projects/xflr5/files/Guidelines.pdf/download (accessed on 26 February 2023)

46. Xing, X. Q., Damodaran, M. Application of Simultaneous Perturbation Stochastic Approximation Method for Aerodynamic Shape Design Optimization. AIAA Journal, 2005, 43(2), 284-294. https://doi.org/10.2514/1.9484

47. Xing, X. Q., Damodaran, M. Assessment of Simultaneous Perturbation Stochastic Approximation Method for Wing Design Optimization. Journal of Aircraft, 2012, 39(2), 379-381. https://doi.org/10.2514/2.2939

48. Xu, W., Li, Y., Pei, B., Yu, Z. A Nonlinear Programming-Based Morphing Strategy for a Variable-Sweep Morphing Aircraft Aiming at Optimizing the Cruising Efficiency. Aerospace, 2023, 10(1), 49. https://doi.org/10.3390/aerospace10010049

49. Yechout, T. R., Morris, S. L., Bossert, D. E., Hallgren W. F. Introduction to Aircraft Flight Mechanics: Performance. Static Stability, Dynamic Stability, and Classical Feedback Control, AIAA Inc., Reston, Virginia, USA, 2003.

50. Yuzhu, L., Wenjie, G., Jin, Z., Yonghong, Z., Donglai, Z., Zhuo, W., Dianbiao D. Design and Experiment of Concentrated Flexibility-Based Variable Camber Morphing Wing. Chinese Journal of Aeronautics, 2022, 35(5), 455-469. https://doi.org/10.1016/j.cja.2021.04.030

51. Zhang, Z. Introduction to Machine Learning: k-nearest Neighbors. Annals of Translational Medicine, 2016, 4(11), 218. https://doi.org/10.21037/atm.2016.03.37